

REVIEW

Synthesis, Characterization and Applications of $\text{MoO}_3\text{-Fe}_3\text{O}_4$ Nanocomposite Material

Madhukar Navgire Akash Nagare Ganesh Kale Sandesh Bhitre*

Jijamata College of Science and Arts, Bhende, Ahmednagar, Maharashtra, India

ARTICLE INFO

Article history

Received: 17 August 2019

Accepted: 21 October 2019

Published Online: 31 October 2019

Keywords:

β -cyclodextrin

Magnetic nanocomposite

Heterogeneous catalyst

Acid-Catalyzed

Organic reactions

ABSTRACT

In the present investigation, a series of nanocomposite material such as MoO_3 , Fe_3O_4 synthesized by co-precipitation method and Beta cyclodextrin (β -CD) doped $\text{MoO}_3\text{-Fe}_3\text{O}_4$ and Graphite doped $\text{MoO}_3\text{-Fe}_3\text{O}_4$ have been synthesized successfully by Sol-Gel method. Synthesized nanomaterials were characterized in detail by XRD, FT-IR, TEM-HRTEM, UV-Vis DRS techniques. The crystalline size was in the range of 10 ± 2 nm. The activity of the prepared material as a heterogeneous catalyst was successfully tested on the organic reaction of synthesis of substituted m-Chloro-Nitrobenzene and it was found to give excellent yield.

1. Introduction

Ferromagnetic nanoparticles have gained considerable importance due to their large surface area, high reactivity, stability and reusability^[1]. The magnetic ionic liquids and magnetizable complex have been used as catalysts in oxidative reaction to enhance separation efficiency^[2-6]. Various Fe_3O_4 based catalyst have been reported by surface modification of zeolites, carbon nanotubes, activated carbon, cyclodextrin etc.^[7-10].

Research has been carried out for the development of supported and un-supported molybdenum, ceria and magnetite nanoparticles^[11-15]. In general, both molybdenum and iron based oxide catalysts have been widely used in many important oxide or acid catalytic reactions

as they are useful in several industrial processes involving organic reactions^[16-20].

The conventional liquid acids and Lewis acids have significant environmental risks. Hence, there is a growing demand for developing eco-friendly strong solid acid catalysts. The inorganic solid acid-catalyzed organic transformations are widely studied because of easy product isolation, high selectivity, easy recovery and recyclability of the catalysts and minimum waste^[21,22]. It has also been observed that metal oxide and mixed metal oxide play an important role in catalytic processes to speed up chemical reactions in an eco-friendly and cost effective manner^[23].

In view of the above facts, this paper deals with the synthesis of MoO_3 and Fe_3O_4 , nanocomposite catalytic

*Corresponding Author:

Sandesh Bhitre,

Jijamata College of Science and Arts, Bhende, Ahmednagar, Maharashtra, India;

Email: sandesh.bhitre@rediffmail.com

material by co-precipitation method and Beta cyclodextrin (β -CD) doped $\text{MoO}_3\text{-Fe}_3\text{O}_4$ and Graphite doped $\text{MoO}_3\text{-Fe}_3\text{O}_4$ nanocomposite catalytic material by Sol-gel method. This is followed with analysis of characterization carried out by XRD, FT-IR, TEM-HRTEM, UV-Vis DRS techniques of the synthesized nanocomposite catalytic material. The synthesized nanocomposite catalyst exhibited high catalytic efficiency for the organic synthesis of substituted m-Chloro-Nitrobenzene and could be quickly separated and recovered by an external magnetic field.

2. Synthesis of Catalyst

The analytical reagents (AR) used for the synthesis were, Ferrous Sulphate (Ranbaxy Fine chemicals), Ferric Sulphate (Ranbaxy Fine chemicals), Ammonium heptamolybdate (Ranbaxy Fine chemicals), Ammonia (SD Fine chemicals), Polyethylene Glycol (SD Fine chemicals), β -Cyclodextrin (β -CD) (Qualigens) and Cetyl Trimethyl Ammonium Bromide (Qualigens) without further purification.

2.1 Synthesis of MoO_3

MoO_3 was synthesized by co-precipitation technique. Ammonium heptamolybdate (2.47 gm) was dissolved in doubled distilled water and then CTAB (1.4 gm) was added to this solution. Then aqueous ammonia (1:1) was added with constant stirring. Excess water was removed by heating the precipitate for 4 hours and dried at 110°C for 2 hours. The material was crushed and calcined at 500°C for 2 hours^[24].

2.2 Synthesis of Fe_3O_4

Fe_3O_4 was synthesized by co-precipitation technique. Fe_3O_4 solution was obtained by dissolving Ferrous Sulphate (2.78gm) and Ferric Sulphate (3.99gm) in distilled water separately and mixed together under vigorously stirring until clear solution was obtained. Then 0.4gm PEG and 1.4 gm. CTAB added into this solution mixed and heated in water bath. Then precipitate was obtained by adding aqueous ammonia solution drop wise (about 10 ml). Excess water was removed by heating the precipitate for 4 hours and dried at 110°C for 2 hours. The material was crushed and calcined at 500°C for 2 hours

2.3 Synthesis of $\text{MoO}_3\text{-Fe}_3\text{O}_4$

$\text{MoO}_3\text{-Fe}_3\text{O}_4$ was synthesized by Sol-gel technique. A solution containing ammonium heptamolybdate (2.47 gm), Ferrous sulphate, (2.78 gm) and Ferric Sulphate (3.99 gm) was mixed with 150 ml distilled water. Cetyl

Trimethyl Ammonium Bromide (2.8 gm) was then added to this solution, mixed and heated in water bath. Then precipitate was obtained by adding aqueous ammonia solution drop wise (about 10 ml). Excess water was removed by heating the precipitate for 4 hours and dried at 110°C for 2 hours. The material was crushed and calcined at 500°C for 2 hours

2.4 Synthesis Of β -CD doped $\text{MoO}_3\text{-Fe}_3\text{O}_4$

β -CD doped $\text{MoO}_3\text{-Fe}_3\text{O}_4$ was synthesized by Sol-gel method. Ferrous sulphate (2.78 gm) and ferric sulphate (3.99 gm) were dissolved in deionized water separately and then mixed together with vigorously stirring. The stirring was continued until a clear solution was obtained. Then 2.470 gm of ammonium heptamolybdate, 1 gm of β -CD, 2.8 gm of CTAB and 1 gm of PVA was added to it. The above solution was then heated in water bath with constant stirring and adding iso-butanol. The pH was maintain at 8 by adding aqueous ammonia drop wise while heating and stirring the mixture for 4 hours at about 1980-2000 RPM. The obtained solution was then dried at 110°C for 2 hour. The material was crushed and calcined at 500°C for 2 hours.

2.5 Synthesis of Graphite doped $\text{MoO}_3\text{-Fe}_3\text{O}_4$

Graphite doped $\text{MoO}_3\text{-Fe}_3\text{O}_4$ was synthesized by Sol-gel method. Deionized water (150 ml) and iso-butanol (10 ml) was mixed thoroughly with ferrous sulphate (2.78 gm), ferric sulphate (3.99 gm), ammonium heptamolybdate (2.47 gm), poly vinyl alcohol (1 gm), CTAB (2.8 gm) and graphite (1 gm). Then it was then constantly stirred at 90°C and ammonia was added drop wise to maintain the pH-8. Excess water was removed by heating the precipitate for 4 hours and dried at 110°C for 2 hours. The material was crushed and calcined at 500°C for 2 hours.

3. Characterizations

3.1 XRD- Analysis

The X-ray diffraction analysis (XRD) of the prepared samples were obtained with a Philips X-ray diffractometer in the diffraction angle range $2\theta^\circ = 20$ to 80 using $\text{CuK}\alpha$ radiation of wavelength 1.5405 \AA .

Figure 1(a) shows the XRD pattern of Fe_3O_4 indicating its crystal structure, phase and lattice modification. The peaks are positioned at $2\theta^\circ = 30.08, 33.73, 37.07, 44.46, 47.15, 50.99, 54.62, 59.23, 63.62$ and 70.95 indicating hkl values due to planes (220), (310), (311), (322), (400), (332), (430), (432), (441) and (620). These peaks

were indexed as cubic Fe_3O_4 as per JCPDS database card number 79-1715 with lattice parameter $a=b=c$ 8.394 Å. Crystallite size calculated by using Debye-Scherrer equation was found to be 8.80 nm^[26].

Figure 1(b) is the XRD pattern obtained of MoO_3 that shows peaks at $2\theta^\circ = 23.33, 25.70, 33.12, 38.83, 42.39, 49.99, 52.83, 62.90, 64.92, 72.87$ and 79.87 corresponding to the planes (110), (040), (101), (060), (141), (230), (080), (251), (190), (232) and (1 11 0) indicating orthorhombic crystal structure. All the peaks are of MoO_3 as matched from the JCPDS card 76-1003^[25] and suggest that the prepared material possess crystalline in nature. The lattice parameters are $a=3.96, b=13.85$ and $c=3.69$ Å and crystallite size was found to be 42.21 nm.

The Figure 1(c) is XRD pattern for β -CD doped $\text{MoO}_3\text{-Fe}_3\text{O}_4$ nanocomposites. The diffraction peaks were observed at $2\theta^\circ = 25.88, 32.72, 42.38, 36.13, 48.95, 54.51, 63.48, 65.49, 72.82$ indexed to hkl planes (122), (400), (503), (035), (414), (718), (441), (531), (443) which indicate the monoclinic symmetry. All the reflection peaks could be indexed to monoclinic symmetry with lattice constants of $a=15.72$ Å, $b=9.24$ Å, and $c=18.22$ Å matched with JCPDS file Card No. 35-0183 are in good agreement with the literature values^[27]. The sharp and distinct peaks suggest that synthesized nanocomposite were highly crystalline, with no impurity peak and are unaffected due to coating with β -CD. The crystallite size was found to be 7.62 nm.

The Figure 1(d) shows that X-Ray diffraction results for graphite doped $\text{MoO}_3\text{-Fe}_3\text{O}_4$ nanocomposites^[28]. All peaks matched the peaks of β -CD doped $\text{MoO}_3\text{-Fe}_3\text{O}_4$ nanocomposites and the diffraction peaks were indexed with JCPDS card 35-0183 and crystallite size was found to be 6.35 nm.

Crystallite size of all samples was calculated by using Debye-Scherrer equation. The crystallite size mentioned is the average of crystallite size calculated using FWHM of three highest intensity peaks.

Table 1. Crystallite size of all samples

Sr. No.	Catalyst	Crystallite Size in nm
1	Fe_3O_4	8.80
2	MoO_3	42.21
3	β -CD doped $\text{MoO}_3\text{-Fe}_3\text{O}_4$	7.62
4	Graphite doped $\text{MoO}_3\text{-Fe}_3\text{O}_4$	6.35

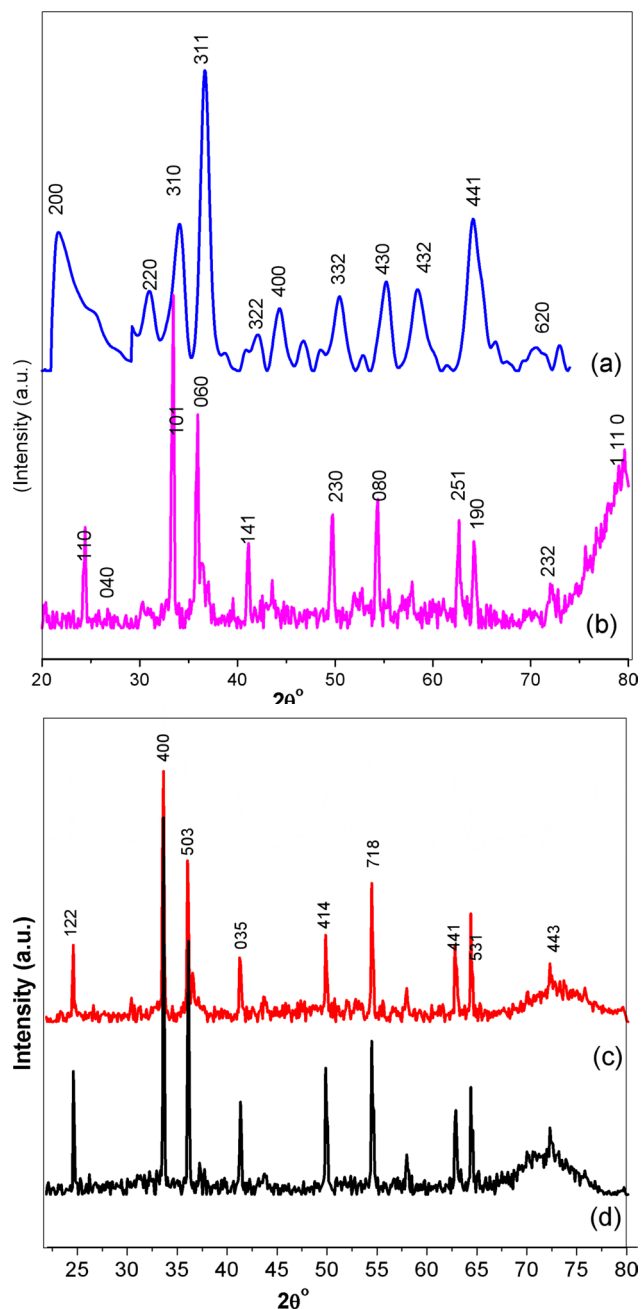


Figure 1. XRD of (a) Fe_3O_4 , (b) MoO_3 , (c) β -CD doped $\text{MoO}_3\text{-Fe}_3\text{O}_4$, (d) Graphite doped $\text{MoO}_3\text{-Fe}_3\text{O}_4$

3.2 FT-IR Analysis

The FT-IR was recorded on FT-IR spectrometer (Perkins Elmer) in the range $4000\text{-}400\text{ cm}^{-1}$. The Figure 2(a) of Fe_3O_4 shows sharp band that appears at 803 cm^{-1} is due to Fe=O bond. The band at 1143 cm^{-1} shows the M-O-M stretching. The Figure 2(b) of MoO_3 shows strong vibrations at 516 cm^{-1} due to the stretching mode of Mo-Mo bonding. Coordinated crystalline water is most likely present as seen from the H-O-H bonding vi-

bration at 1145 cm^{-1} [29].

The Figures 2(c-e) shows the FT-IR spectrum of $\text{MoO}_3\text{-Fe}_3\text{O}_4$, $\beta\text{-CD}$ doped $\text{MoO}_3\text{-Fe}_3\text{O}_4$ and graphite doped $\text{MoO}_3\text{-Fe}_3\text{O}_4$ respectively. The peaks measured for all samples are over the range of $4000\text{-}500\text{ cm}^{-1}$. The peaks at $771, 787, 803\text{ cm}^{-1}$ are because of stretching and bending mode of oxygen in Fe-O-Fe, Mo-O-Mo, Mo=O and Fe=O bonds which indicates the specification of a layered orthorhombic MoO_3 phase and the presence of FeO and Fe_2O_3 . Strong vibrations were detected at $516, 531$ and 539 cm^{-1} which corresponds to formation of bond between $\text{MoO}_3\text{-Fe}_3\text{O}_4$. The band around $1128, 1145, 1120\text{ cm}^{-1}$ is due to co-ordinated crystalline water most likely present due to H-O-H bending vibrations.

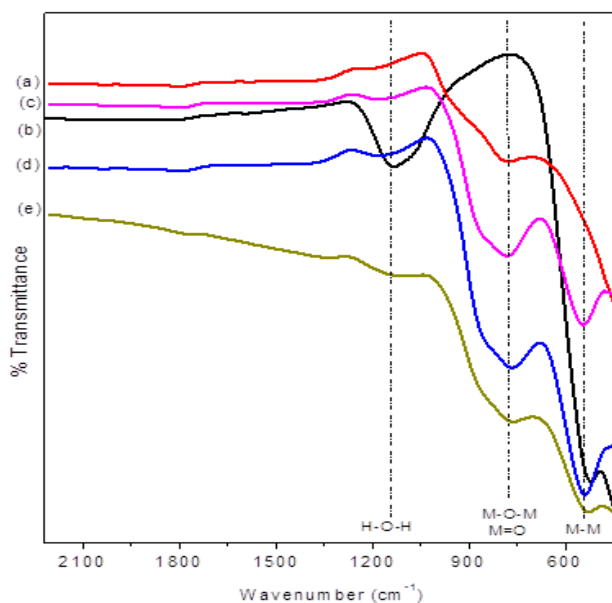


Figure 2. FT-IR spectrums of (a) Fe_3O_4 , (b) MoO_3 , (c) $\text{MoO}_3\text{-Fe}_3\text{O}_4$, (d) $\beta\text{-CD}$ doped $\text{MoO}_3\text{-Fe}_3\text{O}_4$, and (e) graphite doped $\text{MoO}_3\text{-Fe}_3\text{O}_4$

3.3 TEM-HRTEM Analysis

The TEM and HRTEM images were obtained for $\beta\text{-CD}$ doped $\text{MoO}_3\text{-Fe}_3\text{O}_4$, and Graphite doped $\text{MoO}_3\text{-Fe}_3\text{O}_4$. Figure 3(a) for $\beta\text{-CD}$ doped $\text{MoO}_3\text{-Fe}_3\text{O}_4$ exhibits uniform size distribution and high crystalline nature with size range of $10 \pm 2\text{ nm}$, matching with the XRD data which is 8.96 nm . The diffraction spots and rings in SEAD pattern show that the distance from the center of the rings to the diffraction spots are 0.29 nm for (101) planes of MoO_3 and 0.25 nm for (311) planes of Fe_3O_4 .

Figure 3(b) for graphite doped $\text{MoO}_3\text{-Fe}_3\text{O}_4$ also exhibits uniform size distribution and high crystalline

nature with size range of $10 \pm 2\text{ nm}$, matching with the XRD data which is 9.83 nm . The SEAD pattern shows diffraction spots and rings at (101) planes of MoO_3 and (311) planes of Fe_3O_4 .

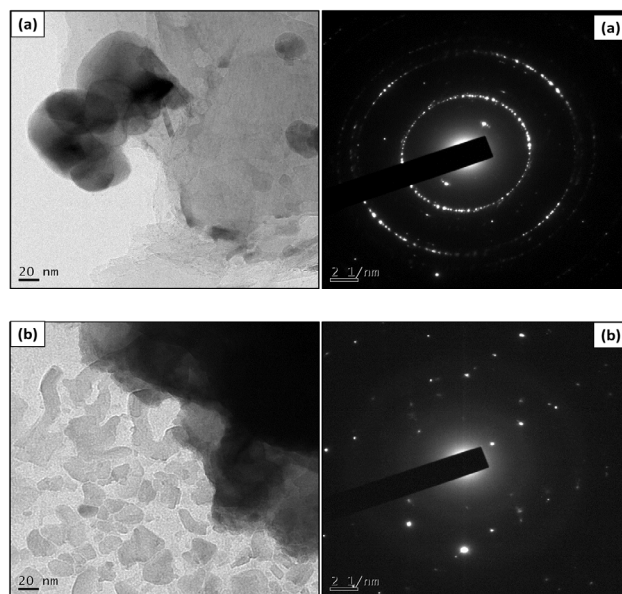


Figure 3. TEM-HRTEM images of (a) $\beta\text{-CD}$ doped $\text{MoO}_3\text{-Fe}_3\text{O}_4$, and (b) Graphite doped $\text{MoO}_3\text{-Fe}_3\text{O}_4$

3.4 UV-Visible DRS Analysis

UV-Visible DRS Analysis was done using Varian Cary (5000) spectrometer in the range of $800\text{-}200\text{ nm}$ and the same are shown in Figure 4. The spectrums show maximum reflectance between $300\text{-}450\text{ nm}$.

The MoO_3 absorbs light of wavelength 351 nm with band gap of around 3.53 eV , Fe_3O_4 absorbs light of wavelength 346 nm with band gap of around 3.58 eV , $\text{MoO}_3\text{-Fe}_3\text{O}_4$ absorbs light of wavelength 348 nm with band gap of around 3.57 eV , $\beta\text{-CD}$ doped $\text{MoO}_3\text{-Fe}_3\text{O}_4$ absorbs light of wavelength 338 nm with band gap of around 3.67 eV and Graphite doped $\text{MoO}_3\text{-Fe}_3\text{O}_4$ absorbs light of wavelength 324 nm with band gap of around 3.83 eV [30]. MoO_3 absorbs light beyond 346 nm due to lower band gap. Interestingly it was observed for modified $\beta\text{-CD}$ doped $\text{MoO}_3\text{-Fe}_3\text{O}_4$ and Graphite doped $\text{MoO}_3\text{-Fe}_3\text{O}_4$ that they absorb of light of wavelengths at 338 nm and 324 nm indicating shift from higher wavelength to lower wavelength that is blue shift. The increase in band gap from 3.53 eV for MoO_3 and 3.58 eV for Fe_3O_4 to 3.67 eV for $\beta\text{-CD}$ doped $\text{MoO}_3\text{-Fe}_3\text{O}_4$ and 3.83 eV for Graphite doped $\text{MoO}_3\text{-Fe}_3\text{O}_4$ indicates greater stability of the doped samples.

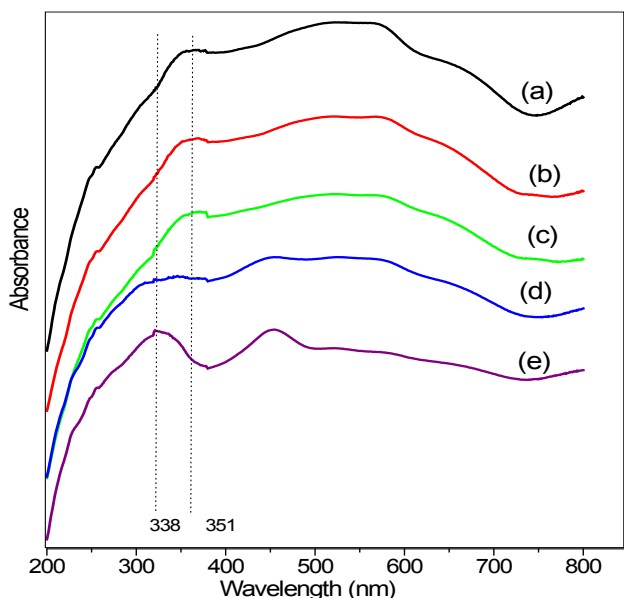
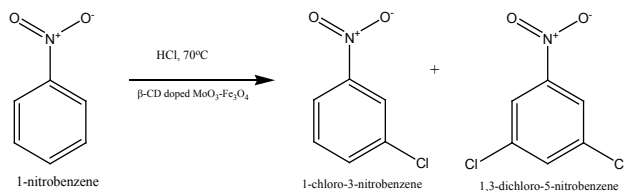


Figure 4. UV-Visible DRS spectrums of (a) MoO_3 , (b) Fe_3O_4 , (c) $\text{MoO}_3\text{-Fe}_3\text{O}_4$, (d) $\beta\text{-CD}$ doped $\text{MoO}_3\text{-Fe}_3\text{O}_4$, and (e) graphite doped $\text{MoO}_3\text{-Fe}_3\text{O}_4$

4. Catalytic Activity Results

The catalytic activity of the synthesized material was examined considering the model reaction of nucleophilic one-pot substitution reaction. The reaction of nitrobenzene (1.0 mmol) with concentrated hydrochloric acid and 0.1 g of catalyst in ethyl alcohol (10 mL) as solvent was carried out at 70°C . The Table 2 shows effect of catalyst on substitution reaction. Among the catalysts $\beta\text{-CD}$ doped $\text{MoO}_3\text{-Fe}_3\text{O}_4$ exhibited very good activity in the synthesis of substituted m-Chloro-Nitrobenzene with excellent yield in very short reaction time as compared to the others. This is attributed to the nano-crystalline size and high porosity of $\beta\text{-CD}$ doped $\text{MoO}_3\text{-Fe}_3\text{O}_4$. In this reaction 93% conversion was observed in 120 minutes which is better in comparison with earlier reported methods.

The predicted mechanism for synthesis of substituted m-Chloro-Nitrobenzene by using $\beta\text{-CD}$ doped $\text{MoO}_3\text{-Fe}_3\text{O}_4$ catalyst is presented in Scheme 1.



Scheme 1. Proposed Mechanism for the preparation of substituted m-Chloro-Nitrobenzene

Table 2. Effect of catalyst on substitution reaction

Entry	Catalyst	Time in minute	Yield/%
1	No Catalyst	No product	0
2	MoO_3	180	78
3	Fe_3O_4	180	58
4	$\text{MoO}_3\text{-Fe}_3\text{O}_4$	180	64
5	$\beta\text{-CD}$ doped $\text{MoO}_3\text{-Fe}_3\text{O}_4$	120	93, 93, 92 ^a
6	Graphite doped $\text{MoO}_3\text{-Fe}_3\text{O}_4$	180	88

Note: Reaction condition: Nitrobenzene (1.0 mmol), Conc. HCl, catalyst (0.1gm), ethyl alcohol (10 mL), temperature (70°C).

^a Product yield with catalyst reused for third time.

Physical and spectroscopic data

1-chloro-3-nitrobenzene: ^1H NMR (DMSO, 300 MHz) δ : 8.40 (s, $J = 2.0\text{Hz}$ 1H), 8.07 (ddd, $J = 8.0, 2.0$ and 2.0Hz 1H), 7.66 (ddd, $J = 8.0, 2.0$ and 2.0Hz 1H), 7.46 (dd, $J = 8.0\text{Hz}$, 1H); FT-IR (Diamond ATR) ν : 3397, 1594, 1166 and 535 cm^{-1} . $\text{C}_6\text{H}_4\text{ClNO}_2$, Exact Mass: 156.99, Mol. Wt.: 157.55, m/e: 156.99 (100.0%), 158.99 (32.0%), 158.00 (6.6%), 159.99 (2.2%), C, 45.74; H, 2.56; Cl, 22.50; N, 8.89; O, 20.31;

Melting Point = 48°C

5. Conclusion

The nanocomposites of MoO_3 and Fe_3O_4 were synthesized successfully by co-precipitation method whereas those of $\text{MoO}_3\text{-Fe}_3\text{O}_4$, $\beta\text{-CD}$ doped $\text{MoO}_3\text{-Fe}_3\text{O}_4$ and Graphite doped $\text{MoO}_3\text{-Fe}_3\text{O}_4$ were synthesized successfully by Sol-gel method. The characterization was done by sophisticated techniques like XRD, FT-IR, TEM-HRTEM, UV-Vis DRS techniques. It was found that crystalline size for all samples was about $10\pm 2\text{ nm}$. Among the synthesized nanocomposite catalytic materials $\beta\text{-CD}$ doped $\text{MoO}_3\text{-Fe}_3\text{O}_4$ exhibited very good catalytic activity for the synthesis of substituted m-chloro nitrobenzene derivatives in environment friendly conditions with excellent yield in very short reaction time, which is 93% conversion was observed in 120 minutes. The catalyst could be quickly separated and recovered by an external magnetic field.

Acknowledgements

1. University Grants Commission (WRO), New Delhi, for financial support in the form of a Minor Research Project.

2. The Principal, Jijamata College of Science and Arts Bhende, for providing the all required facilities to carry out the work.

References

[1] L.J. Xu, J.L. Wang, dx. Environ. Sci. Technol. 2012, 46: 10145–10153.

DOI: org/10.1021/es300303f

- [2] W. S. Zhu, P. W. Wu, L. Yang, Y. H. Chang, Y. H. Chao, H. M. Li, Y. Q. Jiang, W. Jiang, S. H. Xun, *Chem. Eng. J.*, 2013, 229: 250-256.
- [3] W. Jiang, W. S. Zhu, H. M. Li, J. Xiong, S. H. Xun, Z. Zhao, Q. Wang, *RSC Adv.*, 2013, 3: 2355-2361.
- [4] Y. Nie, Y. X. Dong, L. Bai, H. F. Dong, X. P. Zhang, *Fuel*, 2013, 103: 997-1002.
- [5] Y. Z. Chen, F. W. Zhang, Y. Y. Fang, X. H. Zhu, W. L. Zhen, R. Wang, J. T. Ma, *Catal. Commun.*, 2013, 38: 54-58.
- [6] F. Wang, G. J. Wang, H. J. Cui, W. T. Sun, T. B. Wang, *Mater. Res. Bull.*, 2015, 63: 181-186.
- [7] Y. Zhou, L. Sun, H. Wang, W. Liang, J. Yang, L. Wang, S. Shuan, Investigation on the uptake and release ability of β -cyclodextrin functionalized Fe₃O₄ magnetic nanoparticles by methylene blue, *Materials Chemistry and Physics*, 2016, 170: 83-89.
- [8] C. Pizarro, M. A. Rubio, M. Escudey, M. F. Albornoz, D. Munoz, J. Denardin, J. D. Fabris, Nanomagnetite-Zeolite Composites in the Removal of Arsenate from Aqueous Systems, *J. Braz. Chem. Soc.*, 2015, 26: 1887-1896.
- [9] N. Yang, S. Zhu, D. Zhang, S. Xu, Synthesis and properties of magnetic Fe₃O₄-activated carbon nanocomposite particles for dye removal, *Materials Letters*, 2008, 62: 645-647.
- [10] A.L. Cazetta, O. Pezoti, K.C. Bedin, T.L. Silva, A.P. Junior, T. Asefa, V.C. Almeida, Magnetic Activated Carbon Derived from Biomass Waste by Concurrent Synthesis: Efficient Adsorbent for Toxic Dyes, *ACS Sustainable Chem. Eng.*, 2016, 4: 1058-1068.
- [11] ME Navgire, P Gogoi, B Malleshm, A Rangaswamy, BM Reddy, β -Cyclodextrin supported MoO₃-CeO₂ nanocomposite material as an efficient heterogeneous catalyst for degradation of phenol, *RSC Advances* 2016, 6(34): 28679-28687.
- [12] A Gogoi, M Navgire, KC Sarma, P Gogoi, Fe₃O₄-CeO₂ metal oxide nanocomposite as a Fenton-like heterogeneous catalyst for degradation of catechol, *Chemical Engineering Journal*, 2017, 311: 153-162.
- [13] A Gogoi, M Navgire, KC Sarma, P Gogoi, Highly efficient heterogeneous Fenton activities of magnetic β -cyclodextrin (Fe) framework for Eriochrome black T degradation, *Materials Chemistry and Physics*, 2019, 231: 233-243.
- [14] A Gogoi, M Navgire, KC Sarma, P Gogoi, Synthesis and characterization of β -cyclodextrin coated Fe₃O₄/carbon nanocomposite for adsorption of tea catechin from aqueous solutions, *Indian Journal of Chemical Technology*, 2017, 24(5): 498-507.
- [15] A Gogoi, M Navgire, KC Sarma, P Gogoi, Novel highly stable β -cyclodextrin fullerene mixed valent Fe-metal framework for quick Fenton degradation of alizarin, *RSC Advances*, 2017, 7, 64: 40371-40382.
- [16] J. Haber, *The Role of Molybdenum in Catalysis*, Clima Molybdenum, Ann Arbor, MI, 1981.
- [17] Madhukar E. Navgire and Machhindra K. Lande, Selective Synthesis of 2-Aryl-1-arylmethyl-1H-benzimidazoles Using Carbon doped MoO₃ as an Efficient Heterogeneous Catalyst, *International Journal of Engineering Research & Technology*, 2013, 2(10): 2313-2320.
- [18] Baig, A; Ng, F.T.T. A Single-Step Solid Acid-Catalyzed Process for the Production of Biodiesel from High Free Fatty Acid Feedstocks. *Energy Fuels*, 2010, 24: 4712-4720.
- [19] de Paiva, Jr.J.B; Monteiro, W.R; Zacharias, M.A; Rodrigues, J.A.J; Cortez, G.G. Characterization and catalytic behavior of MoO₃/V₂O₅/Nb₂O₅ systems in isopropanol decomposition. *Braz. J. Chem. Eng.*, 2006, 23: 517-524.
- [20] Rathod, S.B; Lande, M.K; Arbad, B.R. Synthesis, Characterization and Catalytic Application of MoO₃/CeO₂-ZrO₂ Solid Heterogeneous Catalyst for the Synthesis of Benzimidazole Derivatives. *Bull. Korean Chem. Soc.*, 2010, 31: 2835-2840.
- [21] Clark, J.H. *Solid Acids for Green Chemistry*. *Acc. Chem. Res.* 2002, 35: 791-797.
- [22] Okuhara, T. *Water-Tolerant Solid Acid Catalysts*. *Chem. Rev.* 2002, 102: 3641-3666.
- [23] Lande, M.K; Navgire, M.E; Rathod, S.B; Katkar, S.S; Yelwande, A.A; Arbad B.R. An efficient green synthesis of quinoxaline derivatives using carbon-doped MoO₃-TiO₂ as a heterogeneous catalyst. *J. Ind. Eng. Chem.* 2012, 18: 277-282.
- [24] M Navgire, M Lande, A Gambhire, S Rathod, D Aware, S R Bhitre, Nanocomposite materials and its photocatalytic activity *Bull. Mater. Sci.*, 2011, 34(3): 535-541.
- [25] Kihlberg L, *Ark. Kemi.* 1963, 21: 557.
- [26] Taylor, *X-ray metallography*, New York: John Wiley, 1961, 678.
- [27] Qin Zhou, Shurong Fu, Min Zou, Yiming He, Ying Wu and Tinghua Wu, *RSC Adv.*, 2015,5: 69388-69393.
- [28] V. Massarotti et al, *J. Appl. Crystallogr.* 1981, 14, 64.
- [29] A.Z.M. Badruddoza, A.S.H. Tay, P.Y. Tan, K. Hidayat, M.S. Uddin, Carboxymethyl- β -cyclodextrin conjugated magnetic nanoparticles as nano-adsorbents for removal of copper ions: synthesis and adsorption studies, *J. Hazard Mater.* 2011, 185: 1177-1186.
- [30] C. Hui, C. Shen, T. Yang, L. Bao, J. Tian, H. Ding, C. Li, H.J. Gao, Large-scale Fe₃O₄ nanoparticles soluble in water synthesized by a facile method, *J. Phys. Chem. C*, 2008, 112: 11336-11339.